SERS Fingerprints of Glutathione, L-arginine, L-histidine, L-tryptophan, Riboflavin metabolites, compared to Raman spectra

SERS Fingerprints of Glutathione, L-arginine, L-histidine, L-tryptophan, Riboflavin metabolites, compared to Raman spectra

Amelia Carolina Sparavigna

Department of Applied Science and Technology, Polytechnic University of Turin, Turin, Italy

Torino, 7 Dicembre, 2024, amelia.sparavigna@polito.it

DOI: https://doi.org/10.5281/zenodo.14290137

Abstract: Here we consider the fingerprints of the SERS spectra of Glutathione, L-arginine, L-histidine, L-tryptophan, Riboflavin metabolites, published by Sherman et al. in Talanta, 2020, in an article entitled "A surface-enhanced Raman spectroscopy database of 63 metabolites", for comparison with the Raman spectral fingerprints of the same molecules, published by De Gelder et al., 2007, in their "Reference database of Raman spectra of biological molecules". The SERS fingerprints are obtained by means of q-Gaussian deconvolutions and Fityk software.

Introduction

In Sparavigna 2023, we proposed the analysis of SERS spectra of L-cysteine, cysteamine, homocysteine metabolites, spectra which have been kindly provided by Sherman et al., 2020. The aim was to investigate the line shapes of SERS peaks by means of q-Gaussian functions; these functions are fundamental for any deconvolution of Raman spectra, as shown by several analyses (Sparavigna, 2023, 2024). In November 2023, we proposed the fingerprints of further metabolites from Sherman et al., to show the relevance of gaining information from them. The fingerprints had been derived from spectra according to a method based on the first derivative behavior, that is on the "first derivative spectrum" (Mosier-Boss et al., 1995). Recently, we submitted for publication the "Atlas" of fingerprints of the Sherman and coworkers' 63 SERS spectra of metabolites, all obtained by means of q-Gaussian deconvolutions. The used software is Fityk. Here, we compare some of these fingerprints, those of Glutathione, L-arginine, L-histidine, L-tryptophan, Riboflavin, with the Raman spectral fingerprints published by De Gelder et al., 2007, in their "Reference database of Raman spectra of biological molecules".

Let us remember that the first use of the term "fingerprint" in relation to the Raman spectroscopy, to the best of my knowledge, is in an article published in 1947 about the Raman spectra of hydrocarbons by Fenske and coworkers. Fenske et al., 1947, wrote that the bands of the Raman spectrum, "which are called Raman lines, are characteristic of the substance illuminated and are therefore a "fingerprint" of that substance". From that time on, the points of identification, such as positions of peaks, shoulders and valleys create the characteristic spectral pattern which is known as the "Raman fingerprint" of a given material. This pattern allows the material classification, "without any preliminary information about composition and structural origin of the individual features" (D'Ippolito et al., 2015).

Deconvolution of spectra

In a manuscript submitted for publication, entitled "Atlas of Metabolite SERS Fingerprints …", using the data kindly provided by Sherman et al., pmc.ncbi.nlm.nih.gov, we propose the fingerprints of metabolites by means of q-Gaussian deconvolutions. Deconvolutions are obtained using Fityk software (Wojdyr, 2010). The q-Gaussians are defined by Sparavigna in a script for this software. Baseline corrections are necessary to avoid negative values of intensity.

The q-Gaussian line shape is a function based on the Tsallis q-form of the exponential function (Tsallis, 1988). This exponential form is characterized by a q-parameter. When q is equal to 2, we have the Lorentzian function. If q is close to 1, we have a Gaussian function. For values of q between 1 and 2, we have a bell-shaped symmetric function with power-law wings ranging from Gaussian to Lorentzian tails.

The q-Gaussian is given as $f(x) = Ce_q(-\gamma x^2)$, where $e_q(.)$ is the q-exponential function and C a scale constant (Hanel et al., 2009). The q-exponential has expression: $e_q(u) = [1 + (1-q)u]^{1/(1-q)}$. For spectroscopy, we write the q-Gaussian function with the center of the band at x_o:

$$q\text{-}Gaussian = Cexp_q(-\gamma(x-x_o)^2) = C\,[1+(q-1)\gamma(x-x_o)^2]^{1/(1-q)}.$$

We can apply q-Gaussian functions by means of Fityk software. In Fityk, a q-Gaussian function can be defined in the following manner:

```
define Qgau(height, center, hwhm, q=1.5) = height*(1+(q-1)*((x-center)/hwhm)^2)^(1/(1-q))
```

where q=1.5 is the initial guessed value of the q-parameter. Parameter hwhm is the half width at half maximum of the line, in the case of a Lorentzian function. In fact, when q=2, the q-Gaussian turns into a Lorentzian function, that we can find defined in Fityk as:

```
Lorentzian(height, center, hwhm) = height/(1+((x-center)/hwhm)^2)
```

When q is close to 1, the q-Gaussian becomes a Gaussian function.

The use of q-Gaussian functions for Raman line shapes has been proposed for the first time in 2023 by A. C. Sparavigna. Subsequently, the q-Gaussians have been shown as suitable for fitting Raman spectra on many occasions. For applying the q-Gaussians to asymmetric bands, we can define also an asymmetric function, turning the Breit-Wigner-Fano (BWF) function into a q-Breit-Wigner-Fano (q-BWF) function (Sparavigna, 2023).

In the abovementioned Atlas, we provide for each metabolite, a screenshot of Fityk software, where the green dots are data from Sherman et al., 2020, red curves the q-Gaussian components, yellow curve the sum of components. In the lower part of the screenshot, the misfit is given (difference between data and yellow curve. Supplementary material is providing two folders containing the Fityk files name_metabolite.fit and name_metabolite-fingerprint.peaks. The link is https://zenodo.org/records/14283580 and also Mendeley Data, doi: 10.17632/jtcgfwgmnz.1

Many thanks to Sherman and coworkers for providing access to their precious data.

Glutathione

Literature provided by Sherman et al.: Dong and Lam, 2011, and Podstawka et al., 2004.

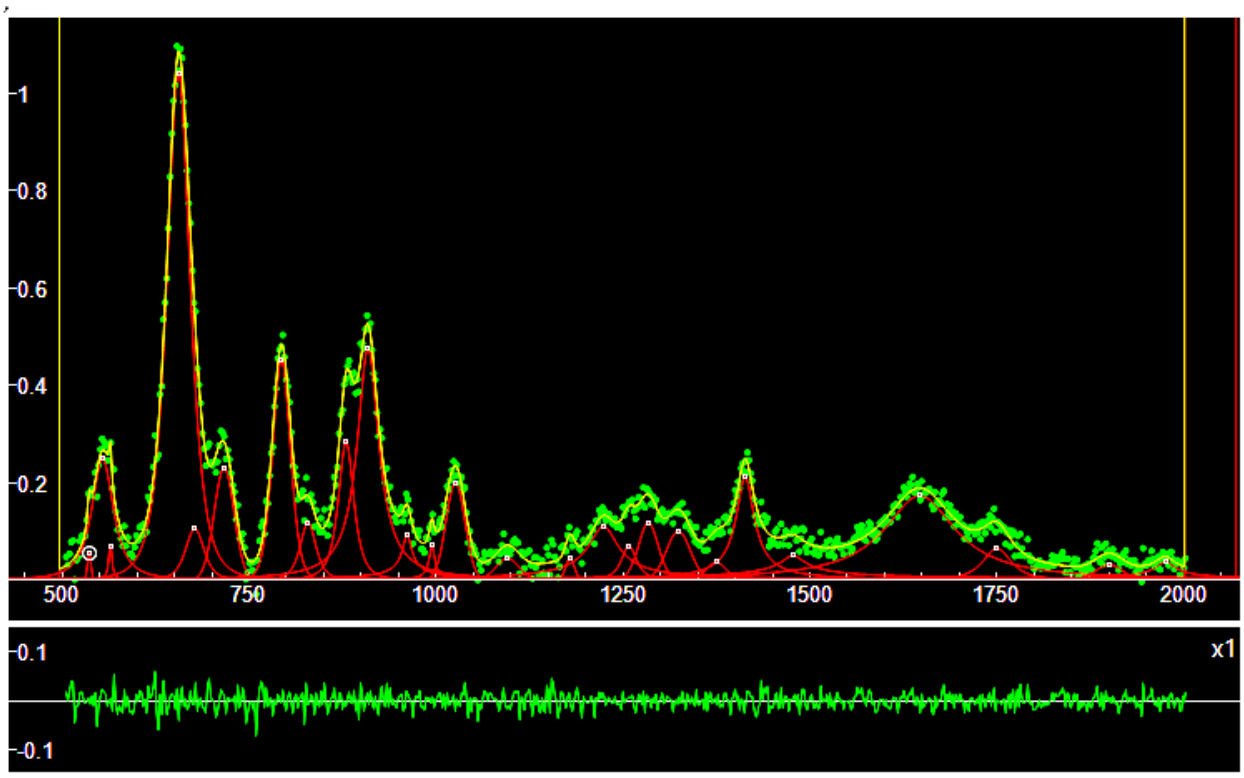

#	PeakType	Center		Parameters	Height	Center	HWHM	q	(height > 0.05)
%_27	Qgau	536.007	x	x	0.0547519	536.007	3.24141	1.00018	
%_5	**Qgau**	**553.927**	**x**	**x**	**0.249743**	**553.927**	**17.8992**	**1.77739**	
%_24	Qgau	564.306	x	x	0.0837745	564.306	2.06509	2.24099	
%_1	**Qgau**	**655.401**	**x**	**x**	**1.04599**	**655.401**	**20.3839**	**1.49549**	
%_16	Qgau	677.241	x	x	0.105765	677.241	16.0279	1.45826	
%_7	**Qgau**	**716.463**	**x**	**x**	**0.230702**	**716.463**	**18.7528**	**0.999787**	
%_3	**Qgau**	**793.173**	**x**	**x**	**0.453925**	**793.173**	**16.3589**	**1.17664**	
%_11	Qgau	828.748	x	x	0.117624	828.748	13.6246	1.52802	
%_4	**Qgau**	**879.585**	**x**	**x**	**0.284483**	**879.585**	**13.0842**	**1.62667**	
%_2	**Qgau**	**909.018**	**x**	**x**	**0.4779**	**909.018**	**17.5125**	**2.02669**	
%_13	Qgau	961.236	x	x	0.0918966	961.236	8.14201	2.95923	
%_25	Qgau	994.473	x	x	0.0708151	994.473	4.53895	2.3707	
%_8	**Qgau**	**1025.87**	**x**	**x**	**0.20019**	**1025.87**	**17.8638**	**0.99994**	
%_14	Qgau	1223.66	x	x	0.110315	1223.66	24.5172	2.50792	
%_22	Qgau	1257.96	x	x	0.0699137	1257.96	12.6826	1.70807	
%_10	Qgau	1283.86	x	x	0.117212	1283.86	18.2406	1.11297	
%_12	Qgau	1323.99	x	x	0.0997824	1323.99	22.6173	0.999256	
%_6	**Qgau**	**1413.39**	**x**	**x**	**0.211364**	**1413.39**	**14.7713**	**2.29633**	
%_9	Qgau	1646.89	x	x	0.173046	1646.89	58.2366	2.0528	
%_15	Qgau	1750.11	x	x	0.0646977	1750.11	23.5459	1.71593	

Here the centers of the q-Gaussian components (in cm^{-1}):

536.007	***553.927(m)***	564.306	***655.401(vs)***	***677.241***	716.463(m)
793.173(s)	***828.748***	879.585(m)	909.018(s)	961.236	994.473
1025.87(m)	***1223.66***	***1257.96***	***1283.86***	1323.99	***1413.39(m)***
1646.89	1750.11				

In De Gelder et al., 2007, we find the following Raman peaks for Glutathione (in bold, the peaks which are corresponding to centers, within +/− 5 cm^{-1}):

400(s), 446(w), 523(w), ***550(m),*** 625(vs), 643(m), ***660(s), 679(vs),*** 722(w), 776(s), 811(m), ***828(m),*** 867(m), 885(s), 917(m), 931(s), 953(m), 972(m), 988(m), 1015(m), 1041(m), 1074(w), 1117(w), 1143(w), 1169(m), ***1224(m),*** 1235(m), ***1255(w), 1280(s),*** 1309(m), 1334(m), 1368(m), 1403(m), ***1415(m),*** 1443(m), 1455(m), 1536(w), 1629(m), 1660(w), 1703(w)

As told by De Gelder and coworkers, "in the spectrum of glutathione, intense bands are related to the presence of the sulphur atom: (1) (C–S) stretching causes intense bands in the region 600–700 cm^{-1} and (2) the band at 400 cm^{-1} can be assigned to υ(C–S) deformations. Furthermore, the (C O) stretching of amide and carboxylic groups gives rise to a broad band at 1630 cm^{-1}".

L-arginine

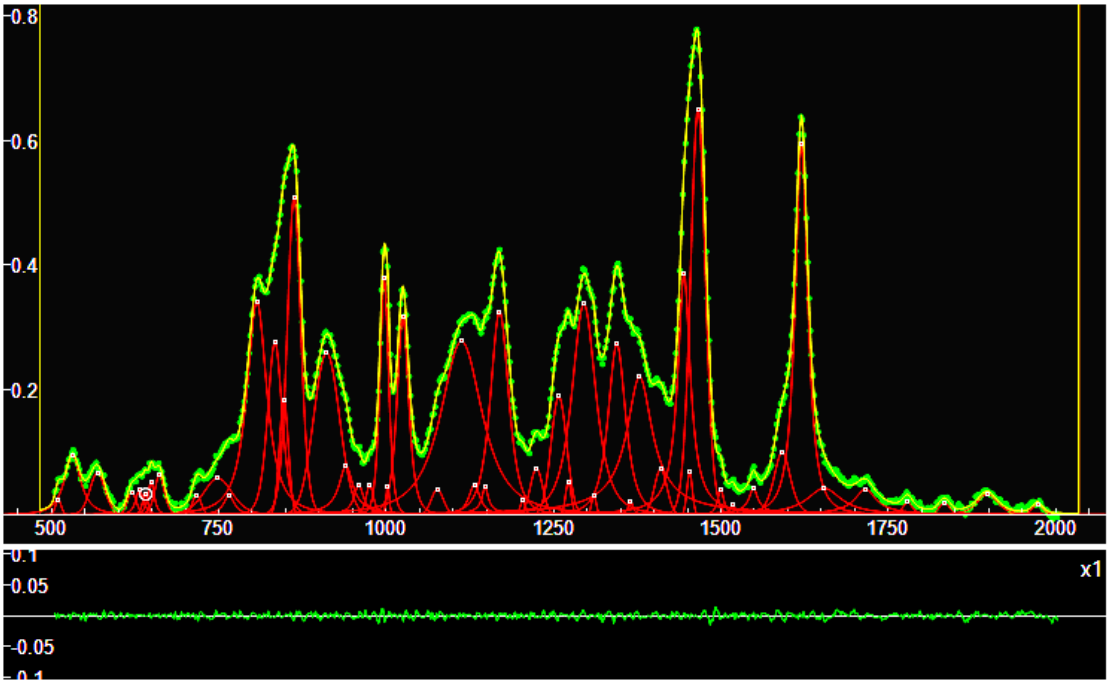

#	PeakType	Center		Parameters	Height	Center	HWHM	q ... (h > 0.05, **bold** h>0.15)
%_18	Qgau	531.445	x	x	0.0965466	531.445	14.87	1.80809
%_22	Qgau	568.693	x	x	0.067613	568.693	15.5271	1.15328
%_60	Qgau	648.893	x	x	0.0537662	648.893	5.80739	1.69304
%_59	Qgau	661.492	x	x	0.0646335	661.492	9.74302	1.31092
%_23	Qgau	748.598	x	x	0.0589676	748.598	29.0783	1.26032

%_9	**Qgau**	**806.805**	**x**	**x**	**0.342536**	**806.805**	**18.4342**	**1.77269**
%_17	**Qgau**	**833.798**	**x**	**x**	**0.277945**	**833.798**	**14.3488**	**1.31045**
%_52	**Qgau**	**847.229**	**x**	**x**	**0.185334**	**847.229**	**9.2883**	**0.999971**
%_51	**Qgau**	**862.433**	**x**	**x**	**0.511955**	**862.433**	**13.59**	**1.20707**
%_12	**Qgau**	**910.998**	**x**	**x**	**0.260015**	**910.998**	**27.1723**	**0.999464**
%_50	Qgau	939.937	x	x	0.0789916	939.937	12.5899	2.22329
%_6	**Qgau**	**997.102**	**x**	**x**	**0.379254**	**997.102**	**8.59164**	**1.35778**
%_58	Qgau	1002.38	x	x	0.0511441	1002.38	2.71727	1.42405
%_10	**Qgau**	**1024.87**	**x**	**x**	**0.320029**	**1024.87**	**11.0673**	**1.51015**
%_11	**Qgau**	**1112.46**	**x**	**x**	**0.278516**	**1112.46**	**38.6364**	**1.70718**
%_5	**Qgau**	**1169.38**	**x**	**x**	**0.326181**	**1169.38**	**17.4575**	**1.53757**
%_24	Qgau	1224.5	x	x	0.0747978	1224.5	13.0212	1.00834
%_13	**Qgau**	**1257.89**	**x**	**x**	**0.190121**	**1257.89**	**16.4587**	**0.999551**
%_32	Qgau	1272.13	x	x	0.0547543	1272.13	5.81358	1.05179
%_8	**Qgau**	**1295.3**	**x**	**x**	**0.338162**	**1295.3**	**22.5636**	**1.58389**
%_7	**Qgau**	**1344.56**	**x**	**x**	**0.274593**	**1344.56**	**16.4393**	**1.6293**
%_14	**Qgau**	**1378.47**	**x**	**x**	**0.221544**	**1378.47**	**23.0369**	**2.27487**
%_21	Qgau	1409.98	x	x	0.0739174	1409.98	13.1975	1.02703
%_15	**Qgau**	**1444.85**	**x**	**x**	**0.387734**	**1444.85**	**11.1535**	**2.06092**
%_41	Qgau	1453.23	x	x	0.0684554	1453.23	5.67164	0.999979
%_2	**Qgau**	**1465.65**	**x**	**x**	**0.652393**	**1465.65**	**15.1134**	**1.12798**
%_16	Qgau	1591.48	x	x	0.100745	1591.48	16.3948	1.352
%_3	**Qgau**	**1620.29**	**x**	**x**	**0.595589**	**1620.29**	**11.7483**	**1.73734**

L-arginine has been investigated in Sparavigna, 2023with the first-derivative spectrum . As told by Sherman et al., SERS spectra of L-arginine have previously been reported in the literature for this molecule, Aliaga et al., 2010, Garrido et al., 2013. Let us add Botta and Bansal, 2015, Dummitt, 2023.

Here the centers of the q-Gaussian components (in bold the strong and medium components):

531.445	568.693	648.893	661.492	748.598	806.805
833.798	***847.229***	862.433	910.998	939.937	997.102
1002.38	1024.87	1112.46	1169.38	1224.5	1257.89
1272.13	***1295.3***	1344.56	***1378.47***	1409.98	1444.85
1453.23	1465.65	1591.48	1620.29		

In De Gelder et al., 2007, we find the following Raman peaks (in bold, the peaks which are corresponding to centers, within +/− 5 cm^{-1}):

376(w), 410(w), 490(mw), 551(m), 577(m), 613(m), ***849(m),*** 879(mw), 922(m), 982(vs), 1036(mw), 1067(s), 1100(m), 1122(m), 1189(m), 1264(mw), ***1298(m),*** 1330(m), ***1377(mw),*** 1436(s), 1475(m), 1713(w)

L-Histidine

Sherman and coworkers propose as literature: Stewart and Fredericks, 1999, Lim et al., 2008, Martusevičius et al., 1996.

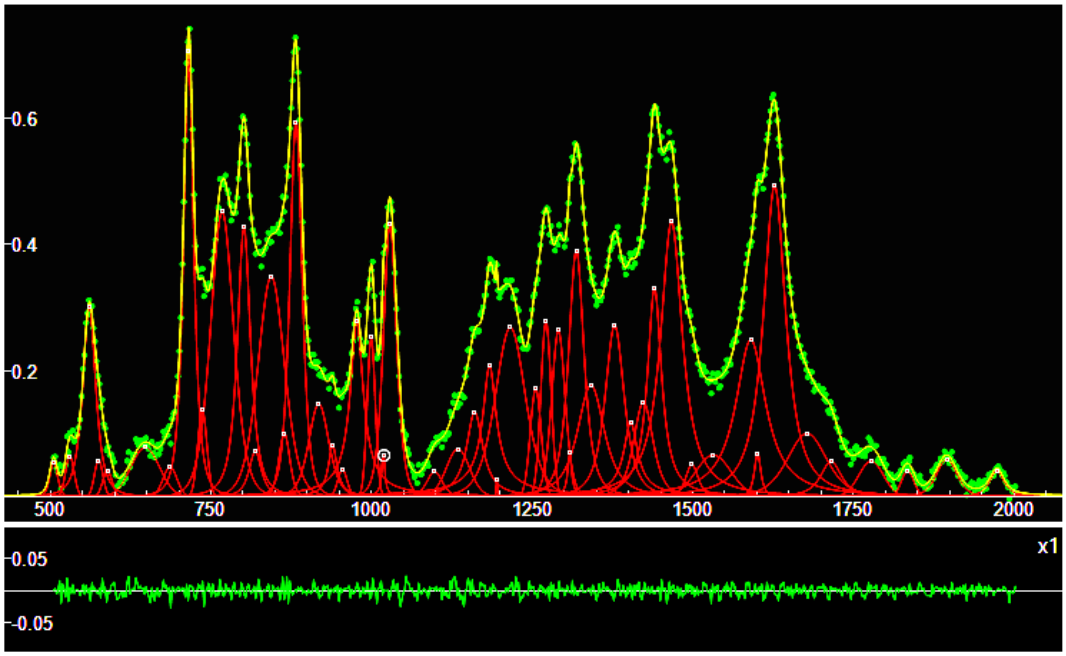

#	PeakType	Center		Parameters	Height	Center	HWHM	q (h > 0.1)
%_17	**Qgau**	**560.408**	**x**	**x**	**0.301956**	**560.408**	**12.8061**	**1.63981**
%_1	**Qgau**	**715.172**	**x**	**x**	**0.71107**	**715.172**	**10.0375**	**1.61021**
%_34	Qgau	736.561	x	x	0.137551	736.561	10.0535	1.00014
%_8	**Qgau**	**767.334**	**x**	**x**	**0.452209**	**767.334**	**24.1083**	**1.26779**
%_5	**Qgau**	**801.304**	**x**	**x**	**0.428227**	**801.304**	**12.6506**	**1.69634**
%_12	**Qgau**	**843.892**	**x**	**x**	**0.349469**	**843.892**	**28.134**	**1.21357**
%_50	Qgau	864.236	x	x	0.100737	864.236	11.4838	1.24183
%_2	**Qgau**	**882.367**	**x**	**x**	**0.597978**	**882.367**	**12.3898**	**1.42412**
%_25	Qgau	917.819	x	x	0.147573	917.819	20.8349	1.31545
%_46	**Qgau**	**976.972**	**x**	**x**	**0.278196**	**976.972**	**12.203**	**2.24447**
%_45	**Qgau**	**999.425**	**x**	**x**	**0.25302**	**999.425**	**8.7543**	**1.00972**
%_9	**Qgau**	**1028.68**	**x**	**x**	**0.433691**	**1028.68**	**13.5383**	**1.35414**
%_48	Qgau	1160.51	x	x	0.135096	1160.51	15.3214	1.99569
%_13	Qgau	1183.64	x	x	0.209011	1183.64	12.4847	2.48762
%_16	**Qgau**	**1216.02**	**x**	**x**	**0.268593**	**1216.02**	**31.2931**	**1.32521**
%_24	Qgau	1255.5	x	x	0.171643	1255.5	12.0003	0.999855
%_10	**Qgau**	**1271.44**	**x**	**x**	**0.278802**	**1271.44**	**11.2618**	**0.999853**
%_14	**Qgau**	**1290.8**	**x**	**x**	**0.264102**	**1290.8**	**14.1843**	**1.26923**
%_6	**Qgau**	**1318.7**	**x**	**x**	**0.392091**	**1318.7**	**15.0808**	**1.62196**
%_20	Qgau	1341.48	x	x	0.177248	1341.48	26.4153	1.68352
%_49	**Qgau**	**1378.39**	**x**	**x**	**0.272027**	**1378.39**	**18.8562**	**1.62214**
%_51	Qgau	1403.31	x	x	0.11858	1403.31	12.9751	2.34933
%_18	Qgau	1423.13	x	x	0.150462	1423.13	19.6822	1.46038
%_4	**Qgau**	**1440.4**	**x**	**x**	**0.331913**	**1440.4**	**13.2271**	**1.99065**
%_7	**Qgau**	**1466.89**	**x**	**x**	**0.436676**	**1466.89**	**20.5567**	**1.94772**
%_15	**Qgau**	**1590.2**	**x**	**x**	**0.249331**	**1590.2**	**28.3836**	**1.98963**
%_3	**Qgau**	**1627.35**	**x**	**x**	**0.493789**	**1627.35**	**21.2911**	**1.85602**
%_22	Qgau	1677.84	x	x	0.100635	1677.84	40.7983	1.32226

Therefore, the centers of the component are:

560.408 715.172 ***736.561*** 767.334 ***801.304*** 843.892

864.236	882.367	***917.819***	***976.972***	999.425	1028.68
1160.51	1183.64	1216.02	1255.5	***1271.44***	1290.8
1318.7	1341.48	1378.39	***1403.31***	1423.13	1440.4
1466.89	1590.2	1627.35	1677.84		

In De Gelder et al., 2007, we find the following Raman peaks (in bold, the peaks which are corresponding to centers, within +/− 5 cm^{-1}):

404(m), 422(mw,sh), 540(mw), 623(mw), 656(m), 680(w), ***731(mw),*** 784(mw), ***804(m),*** 824(mw), 852(m), ***918(m),*** 929(mw,sh), 963(m), ***976(m),*** 1061(m), 1087(s), 1111(m), 1140(mw), 1174(m), 1224(m), 1250(m), ***1271(s), 1317(vs),*** 1336(m), 1347(m), ***1407(m)***, 1430(m), 1476(mw), 1498(m), 1538(w), 1571(m), 1608(w), 1639(w)

L-tryptophan

Sherman et al. are mentioning the SERS spectra reported in Aliaga et al., 2009, Qu et al., 2012. Let us add Aboltaman et al., 2023, Gao et al., 2023, Xu et al., 2022, Gautam et al., 2022.

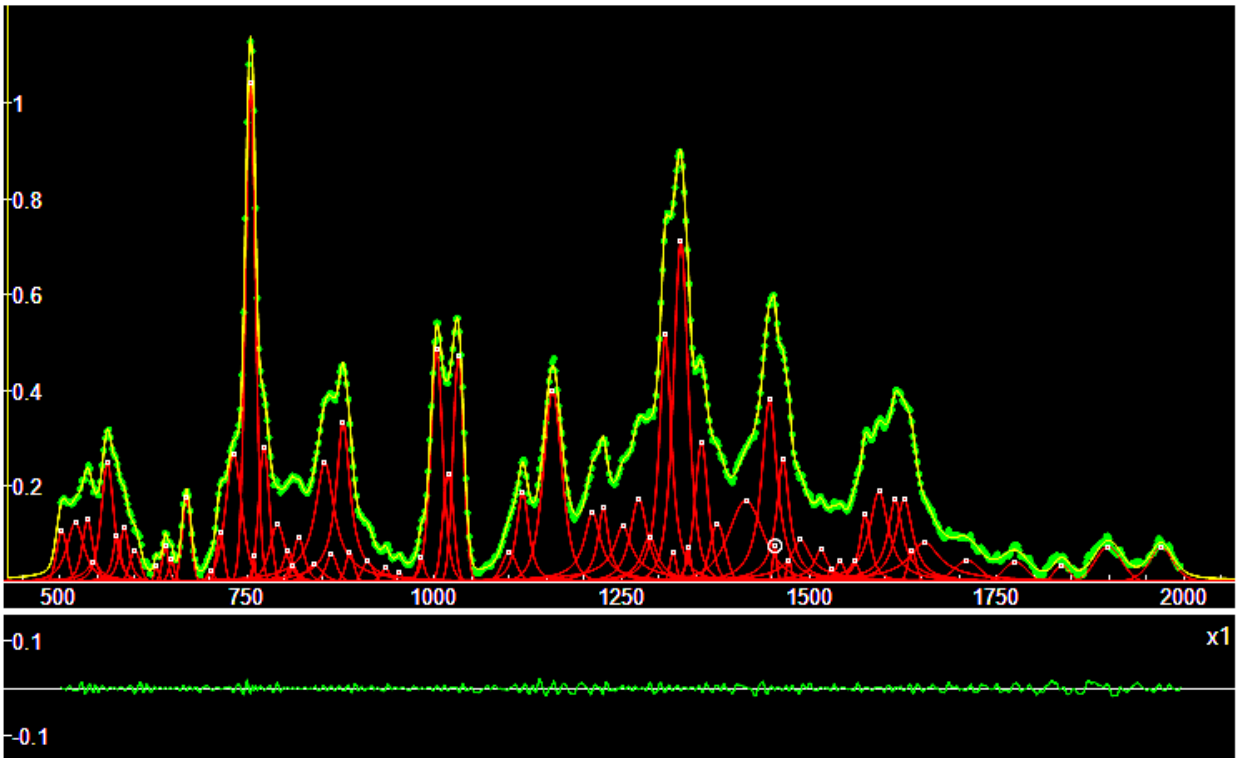

#	PeakType	Center			Parameters	Height	Center	HWHM	q	(h > 0.10, **bold** 0.15)
%_23	Qgau	502.867	x	x	x	0.107574	502.867	9.93948	1.00007	
%_39	Qgau	520.892	x	x	x	0.125706	520.892	14.2531	1.79517	
%_37	Qgau	537.089	x	x	x	0.131668	537.089	8.98731	1.64037	
%_30	**Qgau**	**563.662**	**x**	**x**	**x**	**0.251177**	**563.662**	**10.5553**	**1.55644**	
%_31	Qgau	576.086	x	x	x	0.100255	576.086	5.95915	2.19609	
%_32	Qgau	586.032	x	x	x	0.115546	586.032	7.47295	1.88147	
%_14	**Qgau**	**669.16**		**x**	**x**	**0.178679**	**669.16**	**8.27613**	**1.00002**	

%_25	Qgau	713.926	x	x	x	0.106949	713.926	7.0626	1.00007
%_13	**Qgau**	**732.014**	**x**	**x**	**x**	**0.26742**	**732.014**	**14.3535**	**1.34556**
%_1	**Qgau**	**754.478**	**x**	**x**	**x**	**1.04483**	**754.478**	**9.16089**	**1.09287**
%_2	**Qgau**	**772.585**	**x**	**x**	**x**	**0.282608**	**772.585**	**9.68552**	**1.122**
%_3	Qgau	790.633	x	x	x	0.120398	790.633	13.7032	1.48374
%_46	**Qgau**	**853.641**	**x**	**x**	**x**	**0.250971**	**853.641**	**15.1664**	**2.25154**
%_43	Qgau	878.059	x	x	x	0.337346	878.059	10.8218	2.19526
%_8	**Qgau**	**1002.85**	**x**	**x**	**x**	**0.488488**	**1002.85**	**10.4945**	**1.34517**
%_74	Qgau	1018.32	x	x	x	0.226792	1018.32	10.0937	0.99997
%_49	**Qgau**	**1031.98**	**x**	**x**	**x**	**0.472751**	**1031.98**	**10.0827**	**1.00001**
%_12	**Qgau**	**1117.77**	**x**	**x**	**x**	**0.188738**	**1117.77**	**10.0907**	**1.81205**
%_5	**Qgau**	**1157.77**	**x**	**x**	**x**	**0.400763**	**1157.77**	**16.2389**	**1.43101**
%_50	Qgau	1210.81	x	x	x	0.146988	1210.81	12.7999	2.39824
%_51	**Qgau**	**1225.25**	**x**	**x**	**x**	**0.155778**	**1225.25**	**8.47001**	**2.2198**
%_52	Qgau	1251.39	x	x	x	0.12004	1251.39	13.3395	2.88279
%_18	**Qgau**	**1272.62**	**x**	**x**	**x**	**0.175359**	**1272.62**	**14.1611**	**1.80673**
%_55	**Qgau**	**1308.14**	**x**	**x**	**x**	**0.519178**	**1308.14**	**9.73966**	**1.92027**
%_53	**Qgau**	**1328.8**		**x**	**x**	**0.716256**	**1328.8**	**12.6213**	**1.51458**
%_21	**Qgau**	**1356.39**	**x**	**x**	**x**	**0.292399**	**1356.39**	**11.6362**	**1.40396**
%_28	Qgau	1377.71	x	x	x	0.123692	1377.71	14.1372	1.07609
%_56	**Qgau**	**1415.64**	**x**	**x**	**x**	**0.170769**	**1415.64**	**30.1941**	**1.55756**
%_57	**Qgau**	**1446.99**	**x**	**x**	**x**	**0.382592**	**1446.99**	**12.4754**	**1.95744**
%_58	**Qgau**	**1465.25**	**x**	**x**	**x**	**0.257199**	**1465.25**	**9.85173**	**2.23797**
%_69	Qgau	1574.75	x	x	x	0.141918	1574.75	8.63019	2.02981
%_68	**Qgau**	**1593.2**		**x**	**x**	**0.190361**	**1593.2**	**15.1006**	**2.1287**
%_66	**Qgau**	**1614.92**	**x**	**x**	**x**	**0.173896**	**1614.92**	**11.4481**	**2.3822**
%_67	**Qgau**	**1626.91**	**x**	**x**	**x**	**0.173924**	**1626.91**	**13.5143**	**2.11237**

Therefore, the centers of the components are:

502.867	520.892	***537.089***	563.662	***576.086***	586.032
669.16	713.926	732.014	***754.478 (vs)***	772.585	790.633
853.641	***878.059***	1002.85	1018.32	1031.98	***1117.77***
1157.77	***1210.81***	1225.25	***1251.39***	1272.62	***1308.14***
1328.8 (s)	***1356.39 (s)***	1377.71	1415.64	***1446.99 (s)***	1465.25
1574.75	1593.2	***1614.92***	1626.91		

In De Gelder et al., 2007, we find the following Raman peaks (in **bold**, the peaks which are corresponding to q-Gaussian centers, within +/− 5 cm^{-1}):

393(w), 425(w), 456(w), 498(m), 509(m), ***534(m)***, 548(w), ***574(m),*** 596(m), 626(m), 683(w), 706(m), 741(m), ***755(vs),*** 766(m), 778(m), 802(w), 840(m), 848(m), 865(m), ***874(s),*** 988(w), 1009(vs), 1046(w), 1076(w), 1103(w), ***1118(m), 1160(w), 1207(w),*** 1231(m), ***1253(w),*** 1278(w), ***1309(w),*** 1314(m), ***1328(m),*** 1338(s), ***1358(s),*** 1423(s), ***1450(m),*** 1457(m), 1486(m), 1556(s), ***1576(m), 1616(m)***

Riboflavin

Literature: Liu et al., 2012, Bailey and Schultz, 2016, Dendisová-Vyškovská et al., 2013.

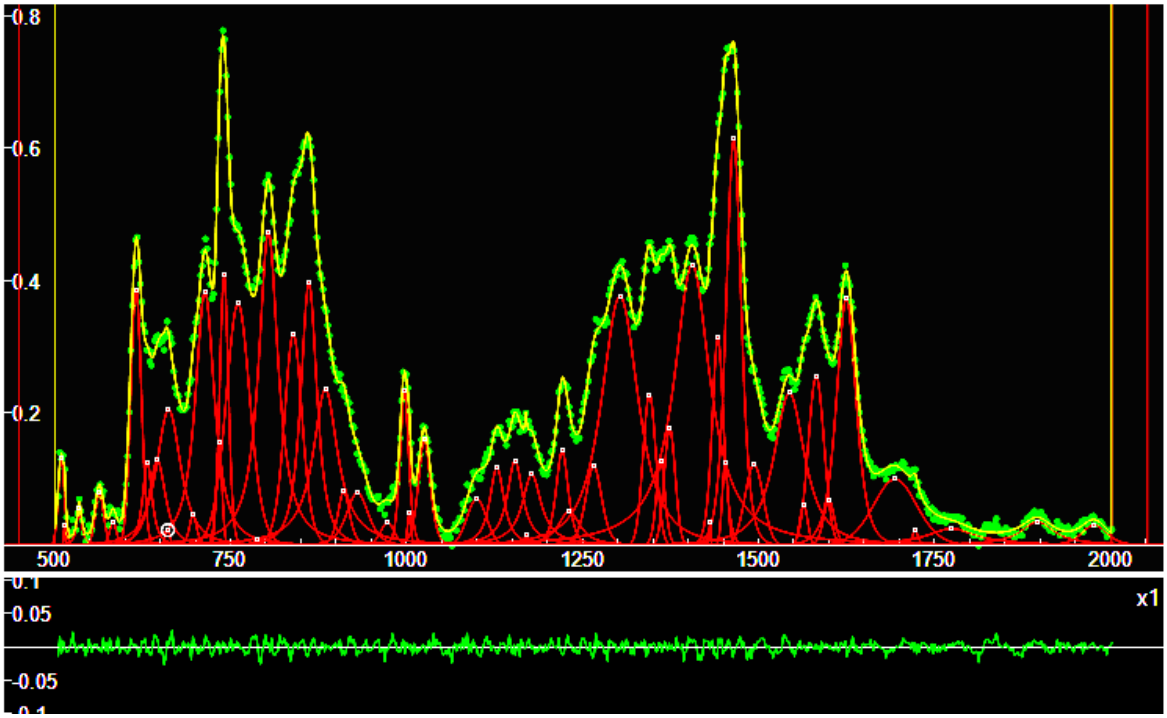

#	PeakType	Center		Parameters	Height	Center	HWHM	q (h>0.13, **bold** h>0.20)
%_20	Qgau	509.548	x	x	0.132844	509.548	6.38009	0.999991
%_6	**Qgau**	**615.63**	**x**	**x**	**0.388069**	**615.63**	**10.6448**	**0.999941**
%_16	**Qgau**	**662.036**	**x**	**x**	**0.205646**	**662.036**	**21.4606**	**1.69231**
%_12	**Qgau**	**713.545**	**x**	**x**	**0.384037**	**713.545**	**16.7399**	**1.78736**
%_33	Qgau	733.814	x	x	0.157629	733.814	5.56765	1.00005
%_1	**Qgau**	**740.705**	**x**	**x**	**0.409706**	**740.705**	**8.39408**	**1.14401**
%_8	**Qgau**	**760.54**	**x**	**x**	**0.365545**	**760.54**	**23.3775**	**1.17989**
%_4	**Qgau**	**803.766**	**x**	**x**	**0.473947**	**803.766**	**16.7303**	**1.91826**
%_9	**Qgau**	**839.139**	**x**	**x**	**0.319764**	**839.139**	**17.2136**	**1.22164**
%_36	**Qgau**	**884.683**	**x**	**x**	**0.236503**	**884.683**	**21.1573**	**2.00948**
%_3	**Qgau**	**861.291**	**x**	**x**	**0.396463**	**861.291**	**14.4233**	**1.65361**
%_14	**Qgau**	**996.936**	**x**	**x**	**0.233248**	**996.936**	**8.18527**	**1.30717**
%_19	Qgau	1025.27	x	x	0.16103	1025.27	11.3529	1.32021
%_21	Qgau	1220.98	x	x	0.143912	1220.98	11.1476	1.51304
%_11	**Qgau**	**1303.11**	**x**	**x**	**0.376702**	**1303.11**	**32.7884**	**1.67156**
%_23	**Qgau**	**1345.03**	**x**	**x**	**0.228627**	**1345.03**	**12.8569**	**1.00495**
%_43	Qgau	1360.9	x	x	0.130955	1360.9	8.24518	1.22131
%_5	Qgau	1373.82	x	x	0.177525	1373.82	11.0558	1.001
%_7	**Qgau**	**1405.66**	**x**	**x**	**0.424245**	**1405.66**	**31.0457**	**1.96519**
%_15	**Qgau**	**1442.17**	**x**	**x**	**0.314003**	**1442.17**	**10.8292**	**1.27372**
%_2	**Qgau**	**1464.65**	**x**	**x**	**0.613821**	**1464.65**	**14.2401**	**1.33739**
%_30	**Qgau**	**1543.71**	**x**	**x**	**0.230789**	**1543.71**	**27.058**	**1.78597**
%_29	**Qgau**	**1581.87**	**x**	**x**	**0.255827**	**1581.87**	**15.8048**	**0.999805**
%_10	**Qgau**	**1624.64**	**x**	**x**	**0.373628**	**1624.64**	**18.3203**	**1.42289**

The centers of the q-Gaussians are:

509.548	615.63	662.036	713.545	733.814	***740.705***
760.54	803.766	839.139	884.683	861.291	996.936

1025.27	1220.98	1303.11	***1345.03***	1360.9	1373.82
1405.66	1442.17	***1464.65***	1543.71	1581.87	***1624.64***

In De Gelder et al., 2007, we find the following Raman peaks (in bold, the peaks which are corresponding to centers, within +/− 5 cm^{-1}):

422(w), 451(w), 502(m), 531(w), 603(w), 677(w), ***742(m),*** 785(m), 1158(m), 1184(m), 1226(s), 1253(w), ***1345(vs), 1402(m), 1464(m),*** 1496(m), 1534(m), 1576(m), ***1621(w),*** 1658(w), 1704(w)

Conclusion

Here we have considered the SERS fingerprints of Glutathione, L-arginine, L-histidine, L-tryptophan, Riboflavin metabolites, published by Sherman et al., 2020, comparing them with the Raman spectral fingerprints of the same molecules, published by De Gelder et al., 2007. The SERS fingerprints have been obtained by means of q-Gaussian deconvolutions and Fityk software. We considered the q-Gaussian centers of SERS deconvolutions and the positions of Raman peaks given by De Gelder and coworkers. It seems that a certain agreement of some components, within +/− 5 cm^{-1}, exists in particular for strong and medium peaks. Further studies are necessary to understand how the peaks are enhanced or suppressed in SERS spectra.

References

1. Aboltaman, R., Kiamehr, Z., Cheraghi, A., & Malekfar, R. (2023). Application of sensitive SERS plasmonic biosensor for high detection of metabolic disorders. Spectrochimica Acta Part A: Molecular and Biomolecular Spectroscopy, 290, 122204.
2. Aliaga, A.E., Garrido, C., Leyton, P., Gomez-Jeria, J.S., Aguayo, T., Clavijo, E., Campos-Vallette, M.M., & Sanchez-Cortes, S. (2010). SERS and theoretical studies of arginine. Spectrochimica Acta Part A: Molecular and Biomolecular Spectroscopy, 76(5), pp.458-463.
3. Aliaga, A.E., Osorio-Roman, I., Garrido, C., Leyton, P., Cárcamo, J., Clavijo, E., Gómez-Jeria, J.S., & Campos-Vallette, M.M. (2009). Surface enhanced Raman scattering study of L-lysine. Vibrational Spectroscopy, 50(1), pp.131-135.
4. Aliaga, A.E., Osorio-Román, I., Leyton, P., Garrido, C., Carcamo, J., Caniulef, C., Celis, F., Díaz F, G., Clavijo, E., Gómez-Jeria, J.S., & Campos-Vallette, M.M. (2009). Surface-enhanced Raman scattering study of L-tryptophan. Journal of Raman Spectroscopy: An International Journal for Original Work in all Aspects of Raman Spectroscopy, Including Higher Order Processes, and also Brillouin and Rayleigh Scattering, 40(2), pp.164-169.
5. Bailey, M. R., & Schultz, Z. D. (2016). SERS speciation of the electrochemical oxidation–reduction of riboflavin. Analyst, 141(17), 5078-5087.
6. Baranska, M., & Proniewicz, L. M. (2008). Raman mapping of caffeine alkaloid. Vibrational Spectroscopy, 48(1), 153-157.
7. Botta, R., & Bansal, C. (2015, June). Surface enhanced Raman scattering (SERS) study of L-arginine adsorbed on Ag nanoclusters on glass substrate by nanocluster deposition method. In AIP Conference Proceedings (Vol. 1665, No. 1). AIP Publishing.
8. Celis, F., Campos-Vallette, M. M., Gómez-Jeria, J. S., Clavijo, R. E., Jara, G. P., & Garrido, C. (2016). Surface-enhanced Raman scattering and theoretical study of the bilichromes biliverdin and bilirubin. Spectroscopy Letters, 49(5), 336-342.

9. Chen, C., Zhang, Y., Wang, X., Qiao, X., Waterhouse, G. I., & Xu, Z. (2024). A core-satellite self-assembled SERS aptasensor containing a “biological-silent region” Raman tag for the accurate and ultrasensitive detection of histamine. Food Science and Human Wellness, 13(2), 1029-1039.
10. Chen, C., Wang, X., Waterhouse, G. I., Qiao, X., & Xu, Z. (2022). A surface-imprinted surface-enhanced Raman scattering sensor for histamine detection based on dual semiconductors and Ag nanoparticles. Food Chemistry, 369, 130971.
11. De Gelder, J., De Gussem, K., Vandenabeele, P., & Moens, L. (2007). Reference database of Raman spectra of biological molecules. Journal of Raman Spectroscopy: An International Journal for Original Work in all Aspects of Raman Spectroscopy, Including Higher Order Processes, and also Brillouin and Rayleigh Scattering, 38(9), 1133-1147.
12. Dendisová-Vyškovská, M., Kokaislová, A., Ončák, M., & Matějka, P. (2013). SERS and in situ SERS spectroscopy of riboflavin adsorbed on silver, gold and copper substrates. Elucidation of variability of surface orientation based on both experimental and theoretical approach. Journal of Molecular Structure, 1038, 19-28.
13. D'Ippolito, V., Andreozzi, G. B., Bersani, D., & Lottici, P. P. (2015). Raman fingerprint of chromate, aluminate and ferrite spinels. Journal of Raman Spectroscopy, 46(12), 1255-1264.
14. Dong, O., & Lam, D. C. (2011). Silver nanoparticles as surface-enhanced Raman substrate for quantitative identification of label-free proteins. Materials Chemistry and Physics, 126(1-2), 91-96.
15. Dummitt, R. (2023). Chemical Effects in Protein Analysis: A Systematic Investigation of Amino Acid Spontaneous Raman and SERS Responses (Doctoral dissertation, The Ohio State University).
16. Fenske, M. R., Braun, W. G., Wiegand, R. V., Quiggle, D., McCormick, R., & Rank, D. H. (1947). Raman spectra of hydrocarbons. Analytical Chemistry, 19(10), 700-765.
17. Gao, F., Grant, E., & Lu, X. (2015). Determination of histamine in canned tuna by molecularly imprinted polymers-surface enhanced Raman spectroscopy, Analytica Chimica Acta 901. 68-75.
18. Gao, W., Duan, W., Peng, D., Li, J., Hu, Z., Wang, D., Gong, Z., & Fan, M. (2023). Surface-enhanced Raman Scattering (SERS) microbial sensor for fresh water acute toxicity monitoring. Microchemical Journal, 191, 108822.
19. Garrido, C., Aguayo, T., Clavijo, E., Gómez-Jeria, J. S., & Campos-Vallette, M. M. (2013). The effect of the pH on the interaction of L-arginine with colloidal silver nanoparticles. A Raman and SERS study. Journal of Raman Spectroscopy, 44(8), 1105-1110.
20. Gautam, R., Chaturvedi, D., Sil, S., Kuhar, N., Singh, S., & Umapathy, S. (2022, September). Characterization of Aggregating Agents towards Sensitive Optical Detection of Tryptophan Using Lab-on-a-Chip. In Photonics (Vol. 9, No. 9, p. 648). MDPI.
21. Hanel, R., Thurner, S., & Tsallis, C. (2009). Limit distributions of scale-invariant probabilistic models of correlated random variables with the q-Gaussian as an explicit example. The European Physical Journal B, 72(2), 263.
22. Jiang, X., Yang, M., Meng, Y., Jiang, W., & Zhan, J. (2013). Cysteamine-modified silver nanoparticle aggregates for quantitative SERS sensing of pentachlorophenol with a portable Raman spectrometer. ACS applied materials & interfaces, 5(15), 6902-6908.
23. Kudelski, A., & Hill, W. (1999). Raman study on the structure of cysteamine monolayers on silver. Langmuir, 15(9), 3162-3168.

24. Lim, J. K., Kim, Y., Lee, S. Y., & Joo, S. W. (2008). Spectroscopic analysis of L-histidine adsorbed on gold and silver nanoparticle surfaces investigated by surface-enhanced Raman scattering. Spectrochimica Acta Part A: Molecular and Biomolecular Spectroscopy, 69(1), 286-289.
25. Liu, F., Gu, H., Lin, Y., Qi, Y., Dong, X., Gao, J., & Cai, T. (2012). Surface-enhanced Raman scattering study of riboflavin on borohydride-reduced silver colloids: Dependence of concentration, halide anions and pH values. Spectrochimica Acta Part A: Molecular and Biomolecular Spectroscopy, 85(1), 111-119.
26. Martusevičius, S., Niaura, G., Talaikyté, Z., & Razumas, V. (1996). Adsorption of L-histidine on copper surface as evidenced by surface-enhanced Raman scattering spectroscopy. Vibrational Spectroscopy, 10(2), 271-280.
27. Mosier-Boss, P. A., Lieberman, S. H., & Newbery, R. (1995). Fluorescence rejection in Raman spectroscopy by shifted-spectra, edge detection, and FFT filtering techniques. Applied Spectroscopy, 49(5), 630-638.
28. Podstawka, E., Ozaki, Y., & Proniewicz, L. M. (2004). Part I: Surface-enhanced Raman spectroscopy investigation of amino acids and their homodipeptides adsorbed on colloidal silver. Applied spectroscopy, 58(5), 570-580.
29. Qu, L. L., Li, D. W., Qin, L. X., Mu, J., Fossey, J. S., & Long, Y. T. (2013). Selective and sensitive detection of intracellular O2•–using Au NPs/Cytochrome c as SERS nanosensors. Analytical chemistry, 85(20), 9549-9555.
30. Qu, L. L., Li, D. W., Xue, J. Q., Zhai, W. L., Fossey, J. S., & Long, Y. T. (2012). Batch fabrication of disposable screen printed SERS arrays. Lab on a Chip, 12(5), 876-881.
31. Sherman, L. M., Petrov, A. P., Karger, L. F., Tetrick, M. G., Dovichi, N. J., & Camden, J. P. (2020). A surface-enhanced Raman spectroscopy database of 63 metabolites. Talanta, 210, 120645.
32. Sparavigna, A. C. (2023). SERS Spectral Bands of L-Cysteine, Cysteamine and Homocysteine Fitted by Tsallis q-Gaussian Functions. International Journal of Sciences, 12(09), 14-24.
33. Sparavigna, A. C. (2023). q-Gaussian Tsallis Line Shapes and Raman Spectral Bands. International Journal of Sciences, 12(03), 27-40.
34. Sparavigna, A. C. (2023). q-Gaussian Tsallis Line Shapes for Raman Spectroscopy (June 7, 2023). SSRN Electronic Journal. DOI: 10.2139/ssrn.4445044
35. Sparavigna A. C. (2023). Tsallis q-Gaussian function as fitting lineshape for Graphite Raman bands. ChemRxiv. Cambridge: Cambridge Open Engage; 2023.
36. Sparavigna, A. C. (2023). Some SERS Fingerprints of Metabolites from the Database Provided by Sherman et al., 2020. Available at SSRN 4634640
37. Sparavigna, A. C. (2023). The Raman Fingerprints of Quartz, Albite and Calcite (October 10, 2023). Available at SSRN 4594641
38. Sparavigna, A. C. (2024). Raman and Attenuated Total Reflectance Infrared RRUFF Spectra: some cases of deconvolution with q-Gaussians and q-BWF functions. Zenodo. https://doi.org/10.5281/zenodo.14220559
39. Sparavigna, A. C. (2024). Atlas of Metabolite SERS Fingerprints obtained by means of q-Gaussian deconvolutions and Fityk Software. Submitted for publication.
40. Sparavigna, A. C. (2024). Metabolite SERS fingerprints: Fityk .fit and .peaks files", Mendeley Data, V1, doi: 10.17632/jtcgfwgmnz.1

41. Stewart, S., & Fredericks, P.M. (1999). Surface-enhanced Raman spectroscopy of peptides and proteins adsorbed on an electrochemically prepared silver surface, Spectrochimica Acta Part A: Molecular and Biomolecular Spectroscopy 55(7) (1999) 1615-1640.
42. Stewart, S., & Fredericks, P.M. (1999). Surface-enhanced Raman spectroscopy of amino acids adsorbed on an electrochemically prepared silver surface, Spectrochimica Acta Part A: Molecular and Biomolecular Spectroscopy 55(7) (1999) 1641-1660.
43. Tsallis, C. (1988). Possible generalization of Boltzmann-Gibbs statistics. Journal of statistical physics, 52, 479-487.
44. Wojdyr, M. (2010). Fityk: a general-purpose peak fitting program. Journal of applied crystallography, 43(5), 1126-1128.
45. Xu, J., Xue, Y., Jian, X., Zhao, Y., Dai, Z., Xu, J., Gao, Z., Mei, Y., & Song, Y. Y. (2022). Understanding of chiral site-dependent enantioselective identification on a plasmon-free semiconductor based SERS substrate. Chemical Science, 13(22), 6550-6557.